doi.org/10.36721/PJPS.2025.38.3.REG.13547.1

Remazolam reduces the activation of hepatic stellate cells by inactivating NOD-like receptor family pyrin domain containing 3/caspase-1/gasdermin D pathway

Jimin He, Run Wang, Pengfei Liu, Yanting Hu and Hui Qiao*
Department of Anesthesiology, Beijing Shijitan Hospital affiliated to Capital Medical University, Beijing, China.

Abstract: Liver fibrosis (LF) is a progressive pathological process driven by hepatic stellate cell (HSC) activation. This study aimed to explore the effect of remazolam (RE), a benzodiazepine anesthetic, on HSC activation and its underlying mechanisms. LX-2 cells were stimulated with lipopolysaccharide (LPS) and treated with various RE concentrations. Cell viability was assessed by CCK-8 assay, and the expression of fibronectin, collagen I, and α-SMA was analyzed via western blot. Pyroptosis was evaluated by morphological observation, LDH release, ELISA for IL-1β/IL-18, and protein expression in the NLRP3/Caspase-1/GSDMD pathway. Rescue experiments were performed by overexpressing NLRP3. RE dose-dependently reduced LX-2 cell viability and downregulated fibronectin, collagen I, and α-SMA expression. RE also significantly inhibited pyroptosis, evidenced by reduced LDH release, decreased IL-1β/IL-18 levels, and suppression of NLRP3, ASC, cleaved caspase-1, GSDMD-N, and IL-1β. Overexpression of NLRP3 reversed the inhibitory effects of RE on pyroptosis and HSC activation. These findings indicate that RE alleviates LF by inhibiting HSC activation and pyroptosis through suppression of the NLRP3/Caspase-1/GSDMD pathway, highlighting its potential as a therapeutic agent for LF.

Keywords: Remazolam; liver fibrosis; NLRP3/caspase-1/GSDMD; pyroptosis

Submitted on 14-10-2024 – Revised on 07-02-2025 – Accepted on 21-04-2025

INTRODUCTION

A fundamental pathological consequence of chronic liver injury (CLI) is liver fibrosis (LF) (Hernaez *et al*., 2020). The remodeling process of LF is continuous and involves several types of cells, inflammatory cytokines and signaling pathway (Campana *et al*., 2021; Khanam *et al*., 2021). In the context of CLI, fibrosis is now recognized as a component of a dynamic process of persistent extracellular matrix (ECM) remodeling, which leads to massive accumulation of multiple extracellular proteins, carbohydrates and proteoglycans (Buakaew *et al*., 2024; Campana *et al*., 2021; Zhao *et al*., 2023). Hepatic stellate cells (HSC) are undoubtedly the primary cells involved in excessive ECM production in LF and their activation is characterized by over expression of recombinant human fibronectin and α-smooth muscle actin (α-SMA) (Higashi *et al*., 2017). Currently, there are no targeted drugs for activated HSC, which limits the development and progress of current anti-fibrotic therapies.

Emerging studies have highlighted that programmed cell death modalities, such as necrosis, apoptosis and pyroptosis, are a hot topic (Murao *et al*., 2021; Shojaie *et al*., 2020). Caspases 1 and Caspases 11 mediate two distinct types of pyroptosis pathways: classical and non-classical routes. This eventually results in the massive production of pro-inflammatory chemicals, such as interleukin-18 (IL-18) and interleukin-1β (IL-1β), which contribute to the development of inflammatory diseases and various liver conditions (Lamkanfi and Dixit, 2014; Murao *et al*., 2021).

Recently, the role of NOD-like receptor family pyrin domain containing 3 (NLRP3) in liver injury has received extensive attention. The inflammasome is an intracellular multiprotein complex that serves as a platform for the release of proinflammatory cytokines. It is composed of pro-caspase-1, apoptosis-associated speck-like protein containing a CARD (ASC) and receptor proteins. A large body of literature has shown that liver diseases, including LF and alcoholic hepatitis, are closely associated with pyroptosis (Guo *et al*., 2019; Knorr *et al*., 2022). For example, unrestricted NLRP3 expression can lead to severe liver inflammatory response, characterized primarily by neutrophil infiltration, HSC excitation and hepatic collagen deposition (Babuta *et al*., 2024; Kui *et al*., 2024; Liu *et al*., 2022). Multiple pathogenic stimuli, such as lipopolysaccharide (LPS), promote HSC activation (Fouts *et al*., 2012). Nuclear factor kappa B (NF-κB) is activated and inflammatory cytokines are produced in response to LPS. They are all involved in HSC activation, chronic inflammation and fibrosis (Ceccarelli *et al*., 2015). In addition, NF-κB is a core mediator of NLRP3 (Zhang *et al*., 2022). Inhibition of the NF-κB/NLRP3 inflammasome passage can reduce LF (Zhao *et al*., 2020). A previous study has demonstrated that inhibition of NF-κB/NLRP3 axis ameliorates ischemic stroke by reducing microglial pyroptosis (Ran *et al*., 2021). Collectively, modulating the activation of NF-κB/NLRP3 inflammatory pathway may

**Corresponding author:* e-mail: docotqh@163.com

limit HSC activation, making it a potential approach for the treatment and prevention of LF.

Remazolam (RE), a novel benzodiazepine drug, exhibits superior pharmacokinetic properties compared to midazolam and other similar drugs, including rapid onset time and faster recovery consciousness (Lee and Shirley, 2021; Wesolowski *et al*., 2016). RE can protect rats from cerebral ischemia/reperfusion (I/R) injury by preventing the occurrence of NLRP3 inflammatory cell pyroptosis (Shi *et al*., 2022). According to a recent study, RE greatly improved the survival rate of septic mice and reduced the production of inflammatory mediators produced by LPS, including IL-6 and TNF-α (Liu *et al*., 2021). Particularly, RE has been demonstrated to alleviate LPS-induced acute liver injury by attenuating inflammatory response (Fang *et al*., 2021). Importantly, RE attenuates inflammation and kidney fibrosis in mice following folic acid injury, as evidenced by decreased collagen deposition, reduced fibroblasts activation and downregulated proinflammatory or profibrotic molecules expression (Song *et al*., 2024). As a new anesthetic, RE is useful in the management of anesthesia in patients with liver cirrhosis (Onoda and Suzuki, 2022). The above evidence suggests that RE is a highly effective and safe sedative that may also have anti-inflammatory and anti-fibrotic actions. The aim of this study was to investigate whether RE could ameliorate LF by regulating HSC activation through blockade of the NLRP3/Caspase-1/GSDMD pathway.

MATERIALS AND METHODS

Cell culture and model building

Human HSC (LX-2) were derived from the Chinese American Type Culture Collection (ATCC; Manassas, VA, USA) cell repository. Cells were maintained in DMEM (Gibco, 11965118, Massachusetts, USA) containing streptomycin-penicillin (Beyotime, C0222, Shanghai, China), 10 mmol/L glutamine and 10% fetal bovine serum (FBS, Excell Bio, FSD500, Suzhou, China). The cells were grown in 5% CO_2 at 37°. After resuspension and counting, the cell density was adjusted. We did not observe significant mycoplasma contamination during cell culture. According to the experimental groups, cells were added to the 96-well plates with 2000 cells per well. Following 24 h, cells were treated with 0, 0.001, 0.01, 0.1 and 1 μg/mL LPS (Thermo Fisher, 00-4976-93, Waltham, USA) for 12 h. Cell viability was examined to determine the optimal stimulation concentration.

Screening for optimal concentration of RE

After selecting the optimal concentration of LPS, the cells were exposed to RE (25, 50 and 100 μM) (MERCK, SML3467, Darmstadt, Germany) for 12 hand cell samples were collected to determine the optimal concentration for medicinal use.

Cell transfection and grouping

The NLRP3 over expression plasmid (pcDNA-NLRP3) was constructed by cloning the full-length human NLRP3 sequence (NM_001079821.3) into the pcDNA3.1 vector (Suzhou Jima Gene Co. Ltd., Suzhou, China), with empty pcDNA3.1 vector serving as the negative control. Plasmid transfection was conducted using Lipofectamine 3000 (Thermo Fisher, L3000001, Waltham, MA, USA) agent. Cells were randomly divided into six groups: (1) Control; (2) LPS (cells treated with LPS for 12 h); (3) LPS + pcDNA (cells transfected with empty pcDNA3.1 vector followed by LPS treatment); (4) LPS + NLRP3 (cells transfected with pcDNA-NLRP3 followed by LPS treatment); (5) LPS + pcDNA + RE (cells transfected with empty vector, then treated with LPS and RE for 12 h); (6) LPS + NLRP3 + RE (cells transfected with pcDNA-NLRP3, then treated with LPS and RE for 12 h). Quantitative reverse transcription (qRT)-PCR was used to assess the transfection efficiency.

Cell counting kit-8 (CCK-8) assay

The successfully transfected or untransfected LX-2 cells were digested and seeded into 96-well plates (2000 cells/well). Finally, CCK-8 solution (Bioss, BA00208, Beijing, China) was added to each well 2 h prior to the termination of incubation (final concentration of CCK-8 was 10%). After incubation, OD450 values were detected using a microplate reader (RT-6000, Rayto, Shenzhen, China).

Lactate dehydrogenase (LDH) release experiment

Following experimental treatments, the LDH release assay was performed according to the manufacturer's protocol (Beyotime, C0016, Shanghai, China). Briefly, the LDH working liquid was prepared and added to each well 1 h prior to measurement. After incubation, the samples were centrifuged in a perforated plate centrifuge and 120 μL of the supernatant was transferred to a 96-well plate. Then, 60 μL LDH working liquid was added to each well. After mixing, the mixture was incubated at 25° in the dark for half an hour. The OD value was measured at 490 nm.

Enzyme-linked immunosorbnent assay (ELISA)

LX-2 was seeded in 6-well plates at a density of 1×10^6 cells per well and subsequently cultured in complete medium containing 10% FBS for 24 h. Following incubation, various reagents were used for washing and color development according to the instructions in the specific kits of IL-1β (Beyotime, PI305e, Shanghai, China) and IL-18 (Beyotime, PI558e, Shanghai, China). The absorbance at 450 nm was measured and the amount of each component in the cell culture supernatant was estimated.

qRT-PCR

The cell precipitations from each group were collected. The total RNA was extracted and assayed for RNA concentration and purity using a kit (Vazyme, RC112, Nanjing, China). RNA was converted to cDNA using the

reverse transcription kit (Vazyme, R312, Nanjing, China). The qRT-PCR kit (Vazyme, Q712, Nanjing, China) was used to test the relative transcript levels based on the CT values. Primers are listed in table 1.

Western blotting (WB)

RIPA lysis buffer (100μL) was added for cell lysis. The BCA assay (NCM Biotech, WB6501, Suzhou, China) was used to quantify the proteins. After separation by SDS-PAGE, the proteins were transferred to polyvinylidene fluoride (PVDF) membranes (Sigma-aldrich, IPVH00010, Missouri, USA). The membranes were incubated in 5% milk (BioFroxx, 1172, Hefei, China). Primary antibodies were applied: Collagen Type I (1:2000, 14695-1-AP, Proteintech, Rosemont, IL, USA), α-SMA (1:4000, 14395-1-AP, Proteintech, Rosemont, IL, USA), GSDMD-N (1:1000, ab215203, Abcam, Cambridge, MA, USA), NLRP3 (1:1000, bs-10021R, Bioss, Wuhan, China), pro-caspase-1 (1μg/mL, 14F468, Invitrogen, Carlsbad, CA, USA), cleaved caspase-1 (1:1000, Asp297, Invitrogen, Carlsbad, CA, USA), GSDMD (1:1000, bs-14287R, Bioss, Wuhan, China), pro-IL-1β (1:1000, 16806-1-AP, Proteintech, Rosemont, IL, USA), ASC (1:2000, 10500-1-AP, Proteintech, Rosemont, IL, USA), mature-IL-1β (1:1000, Asp116, CST, Danvers, MA, USA), fibronectin (1:2000, 15613-1-AP, Wanleibio, Shenyang, China), GAPDH (1:80000, 60004-1-Ig, proteintech, Rosemont, IL, USA). After incubation overnight at 4°, the films were removed and washed with three rounds of TBST (Biosharp, BL315B, Anhui, China). The secondary antibody (1:10000, bs-0296G-HRP/bs-0296G-HRP, Bioss, Wuhan, China) was then placed on the PVDF membranes for 2h (room temperature). Chemiluminescent reagents A and B (NCM Biotech, P2100, Suzhou, China) were mixed and added to the PVDF membranes using uniform drops. The specimens were imaged using a chemiluminescence imager (Jiapeng, JP-K6000, Shanghai, China).

STATISTICAL ANALYSIS

Data were analyzed using Graphpad Prism (Version X; La Jolla, CA, USA). All data were displayed as mean ± standard deviation. The one-way ANOVA test with Tukey's post hoc test was applied for comparisons more than two groups, whereas the *t* test was used for comparisons between two groups. Statistical significance was defined as $P < 0.05$.

RESULTS

Effects of LPS on the activation of LX-2 cells at different concentrations

LX-2 cells were stimulated with varying concentrations (0, 0.001, 0.01, 0.1, 1 μg/mL) of LPS for 12 hand cell viability was examined. The results displayed that LPS dose-dependently increased the viability of LX-2 cells, with 0.1 μg/mL LPS exhibiting the most pronounced effect ($p < 0.05$ or $p < 0.001$; fig. 1A). Consistent with the CCK8 assay results, LPS treatment markedly increased the expression of fibronectin, collagen Type I and α-SMA in LX-2 cells ($p < 0.05$, $p < 0.01$ or $p < 0.001$; fig. 1B-C). Since the 0.1 μg/mL LPS group showed the highest expression levels of these proteins, this concentration was selected for subsequent experiments.

Inhibitory effects of different concentrations of RE on LPS-induced activation of LX-2 cells

To explore the impact of RE on LPS-induced activation of LX-2 cells, we used the same experimental approach as described in the above section. After the above experiments, we found that the optimal concentration of LPS was 0.1 μg/mL, so we used this concentration to establish a model and added different concentrations (25, 50, 100 μM) of RE to LX-2 cells. The results of the CCK8 assay (fig. 2A) showed that 25, 50 and 100 μM RE significantly reduced the viability of LX-2 cells ($p < 0.001$), with the most pronounced inhibitory effect observed at 100 μM. Cell samples were collected and protein levels were detected by WB. These results were consistent with those of the CCK8. The protein expression levels of fibronectin, collagen Type I and α-SMA in LX-2 cells were markedly decreased in RE groups at 25, 50 and 100 μML ($p < 0.05$, $p < 0.01$ or $p < 0.001$; fig. 2B-C). Notably, the 100 μM RE group exhibited the most significant suppression of all three proteins. Therefore, we identified 100 μM as the optimal RE concentration for subsequent experiments.

RE inhibits pyroptosis and the NLRP3/Caspase-1/GSDMD pathway in LX-2 cells

The effect of RE on pyroptosis in LX-2 cells was further examined. First, we observed the cell morphology (fig. 3A) and found that cells in the Control group were spindle-shaped with intact cytoplasm, uniform adherent growth, clear boundaries and clear nuclei. In the LPS-treated group, cells exhibited characteristic pyroptotic features including cellular swelling, irregular contraction patterns, irregular cell shape, unclear nuclei and more dead cells. In contrast, RE treatment significantly ameliorated these morphological changes, with cells exhibiting clearer boundaries, more regular morphology and fewer dead cells compared to the LPS group. LDH release is commonly used to evaluate pyroptosis. As shown in fig. 3B, LPS treatment notably increased LDH release ($p < 0.001$), which was markedly attenuated by RE intervention ($p < 0.001$).

Similarly, ELISA results displayed that the levels of IL-1β and IL-18 in the LPS group were markedly higher than those in the control group ($p < 0.001$; fig. 3C), which were significantly decreased after RE intervention ($p < 0.001$). WB analysis revealed that there were no significant differences in the expression of pro-caspase-1, GSDMD and pro-IL-1β among the control, LPS and LPS + RE groups ($P > 0.05$) (fig. 3D-E).

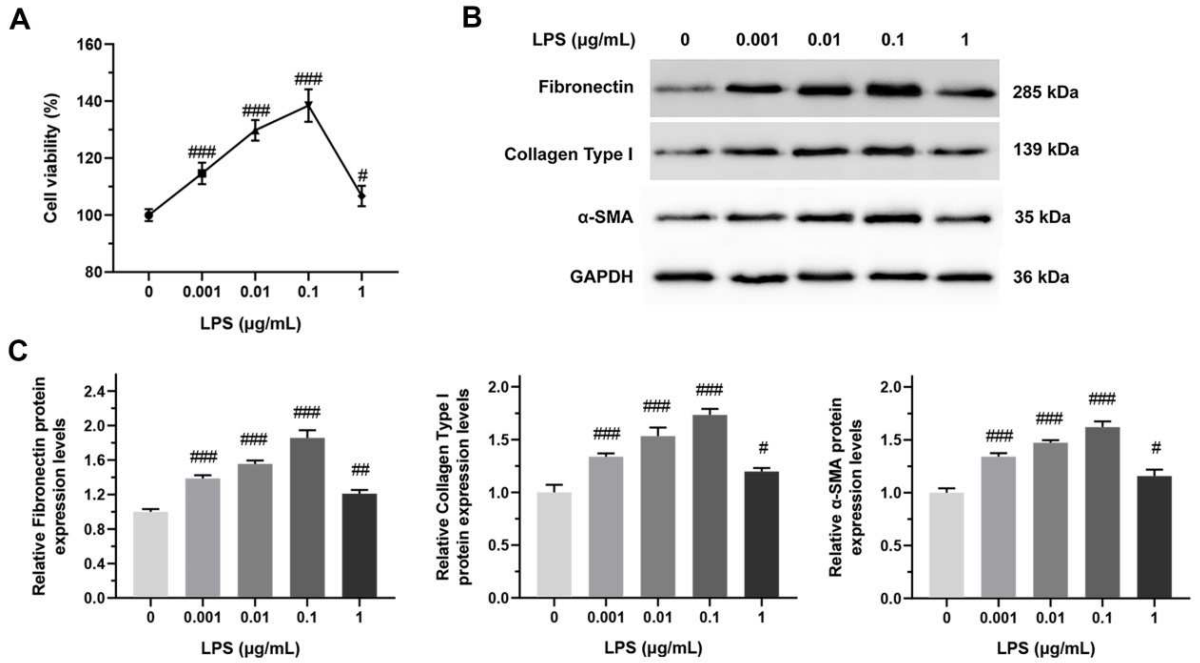

(A) Cell viability was detected using the CCK8 kit. n=6. (B) Representative WB images of fibronectin, collagen Type I and α-SMA. n = 3. (C) The relative quantify of fibronectin, collagen Type I and α-SMA expression assessed by WB. n = 3. $^{\#}p < 0.05$, $^{\#\#}p < 0.01$, $^{\#\#\#}p < 0.001$ vs. 0 μg/mL LPS.

Fig. 1: Effects of LPS on the activation of LX-2 cells at different concentrations.

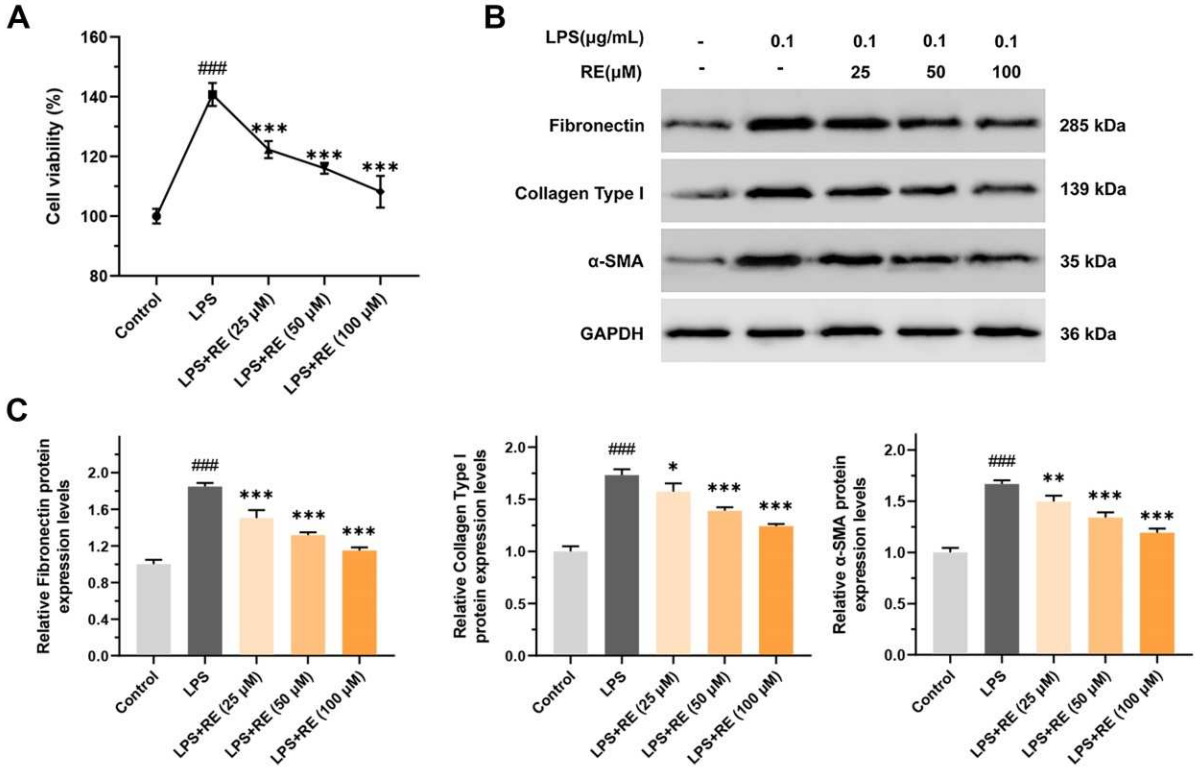

(A) Cell viability was detected using the CCK8 kit. n = 6. (B) Representative WB images of fibronectin, collagen Type I and α-SMA. n = 3. (C) The relative quantify of fibronectin, collagen Type I and α-SMA expression assessed by WB. n = 3. $^{\#\#\#}p < 0.001$ vs. Control; $^{*}p < 0.05$, $^{**}p < 0.01$, $^{***}p < 0.001$ vs. LPS.

Fig. 2: Inhibitory effects of different concentrations of RE on LPS-induced activation of LX-2 cells.

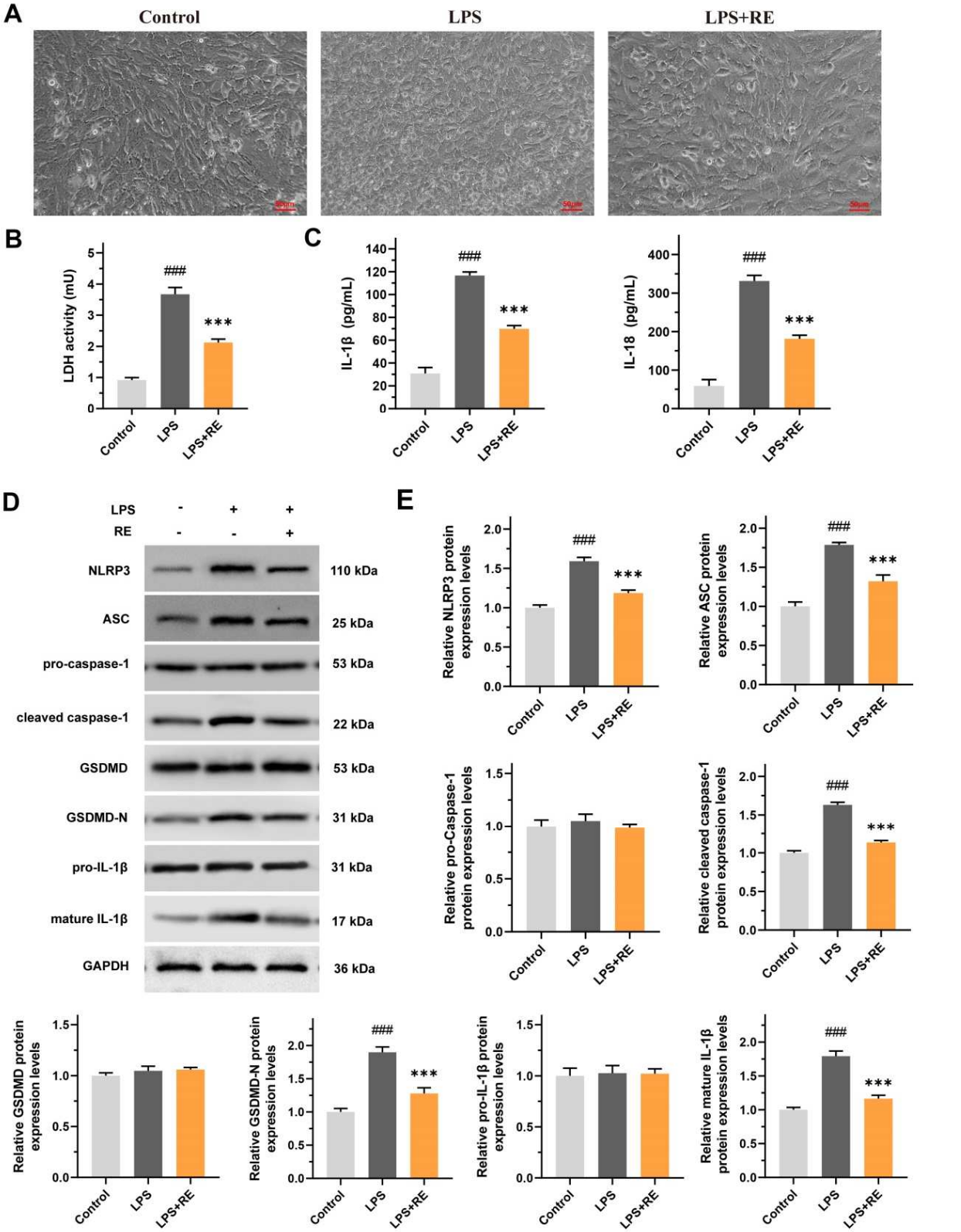

(A) Representative cell morphology observed by inverted microscope. n = 5. (B) LDH release was detected using a commercial kit. n = 6. (C) IL-1β and IL-18 contents were assessed by ELISA. n = 6. (D) Representative WB images of proteins in NLRP3/Caspase-1/GSDMD pathway. (E) The relative quantify of proteins in NLRP3/Caspase-1/GSDMD pathway assessed by WB. n = 3. $^{###}p < 0.001$ vs. Control; $^{***}p < 0.001$ vs. LPS.

Fig. 3: RE inhibits pyroptosis and the NLRP3/Caspase-1/GSDMD pathway in LX-2 cells.

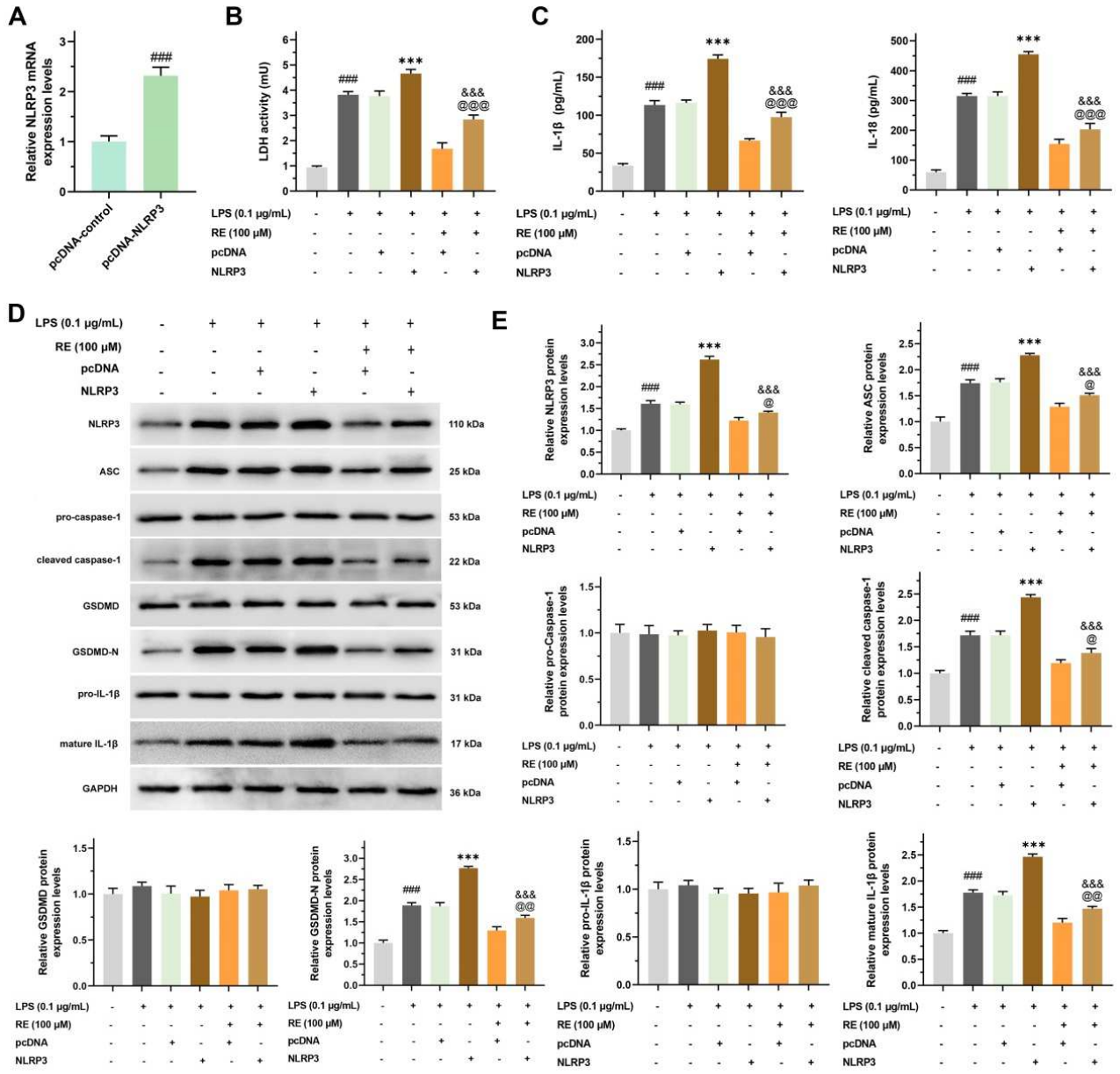

(A) The transfection efficiency of NLRP3 was assessed using qRT-PCR. n = 3. $^{###}p < 0.001$ vs. pcDNA-control. (B) LDH release was detected using a commercial kit. n = 6. (C) IL-1β and IL-18 contents were assessed by ELISA. n = 6. (D) Representative WB images of proteins in NLRP3/Caspase-1/GSDMD pathway. (E) The relative quantify of proteins in NLRP3/Caspase-1/GSDMD pathway assessed by WB. n = 3. $^{###}p < 0.001$ vs. Control; $^{***}p < 0.001$ vs. LPS (0.1 μ(/mL)+pcDNA; $^{@}p < 0.05$, $^{@@}p < 0.01$, $^{@@@}p < 0.001$ vs. LPS (0.1 μg/mL)+RE (100 μ1)+pcDNA; $^{\&\&\&}p < 0.001$ vs. LPS (0.1 μg/mL)+NLRP3.

Fig. 4: NLRP3 overexpression counteracts the inhibitory effect of RE on LX-2 cell pyroptosis.

Compared to the control group, the LPS group had markedly increase in the expression of NLRP3, ASC, cleaved caspase-1, GSDMD-N and IL-1β ($p < 0.001$). Conversely, the RE-treated cells exhibited markedly reduction in the expression of these proteins ($p < 0.001$). These findings demonstrated that RE could inhibit pyroptosis and that activation of the NLRP3/Caspase-1/GSDMD pathway may be involved.

NLRP3 over expression counteracts the inhibitory effect of RE on LX-2 cell pyroptosis

In order to further investigate whether RE inhibits pyroptosis by restraining the NLRP3/Caspase-1/GSDMD pathway, we first evaluated NLRP3 over expression efficiency. Results showed that the NLRP3 mRNA expression in the pcDNA-NLRP3 group was dramatically greater than that in the pcDNA group ($p < 0.001$; fig. 4A). Assessment of pyroptosis markers revealed no significant differences in LDH activity and IL-1β and IL-18 contents between LPS (0.1 μg/mL)+pcDNA and LPS (0.1 μg/mL) groups ($P > 0.05$; fig. 4B-C), indicating that the empty pcDNA vectors had no effect on cells. These indices were

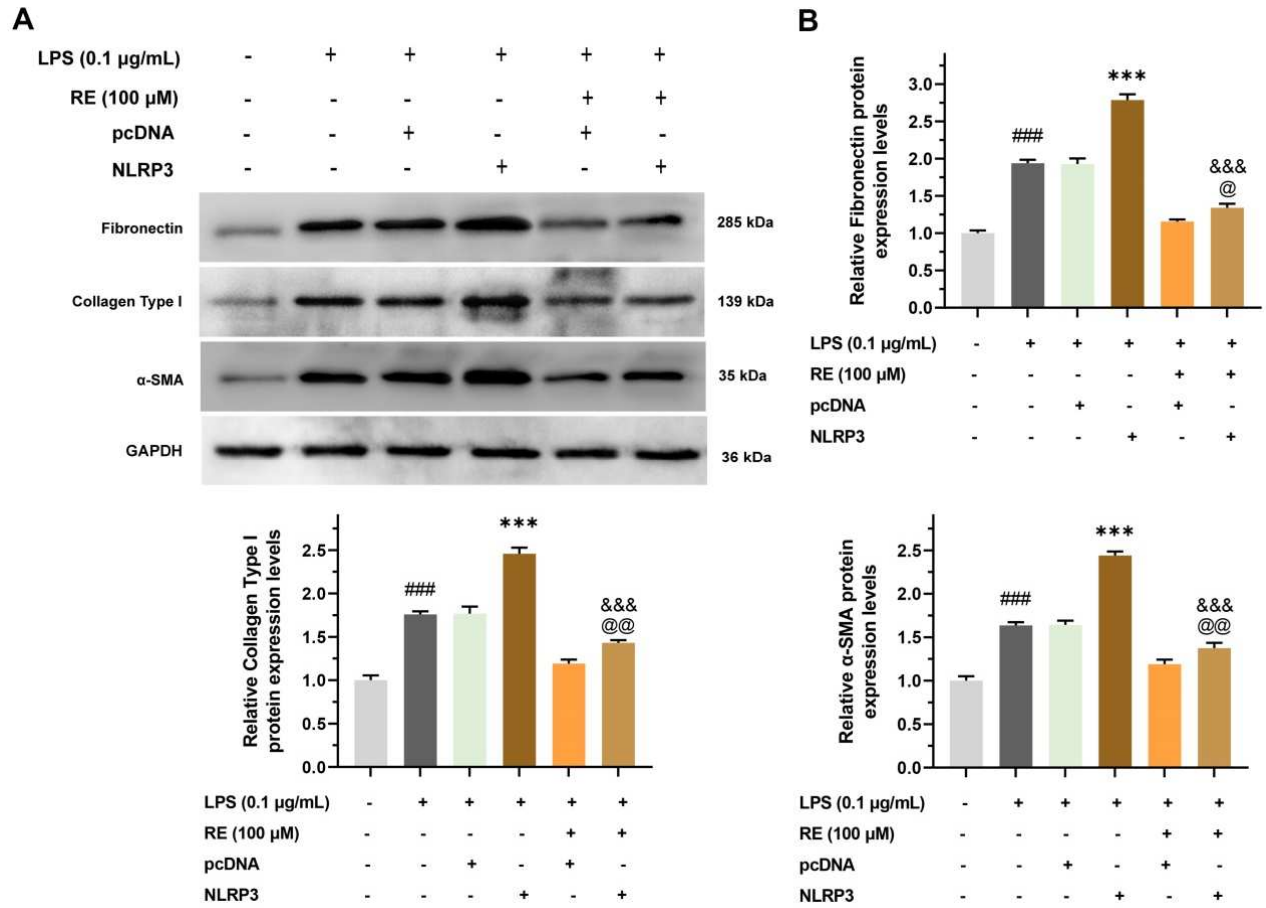

(A) Representative WB images of fibronectin, collagen Type I and α-SMA. n = 3. (B) The relative quantify of fibronectin, collagen Type I and α-SMA expression assessed by WB. n = 3. $^{###}p < 0.001$ vs. Control. $^{***}p < 0.001$ vs. LPS (0.1 μg/mL)+pcDNA; $^{@}p < 0.05$, $^{@@}p < 0.01$ vs. LPS (0.1 μg/mL)+RE (100 μM)+pcDNA; $^{\&\&\&}p < 0.001$ vs. LPS (0.1 μg/mL)+NLRP3.

Fig. 5: Overexpression of NLRP3 reverses the inhibitory effect of RE on LX-2 cell activation.

Table 1: Primer sequences for qRT-PCR

Gene	Species		Sequences (5'-3')
NLRP3	Human	Forward	TAGCCTTGTCAGATAAGGAAGGAACAGCTTCACAGTCAACTTTGT
		Reverse	ACAGCTTCACAGTCAACTTTGT
GAPDH	Human	Forward	CGCTAACATCAAATGGGGTGTGCCAGCCCCAGCGTCAAAG
		Reverse	TGCCAGCCCCAGCGTCAAAG

markedly higher in the LPS (0.1 μg/mL)+NLRP3 group than that in the LPS (0.1 μg/mL)+pcDNA group ($p < 0.001$)and those in the LPS (0.1 μg/mL)+RE (100 μM)+pcDNA group were markedly lower than those in the LPS (0.1 μg/mL)+pcDNA group ($p < 0.001$). In addition, NLRP3 over expression abolished the suppressive effect of RE on pyroptosis in LX-2 cells. Next, the WB assay results manifested that there were no significant difference in the protein expression of pro-caspase-1, GSDMD and pro-IL-1β among the groups ($P > 0.05$; fig. 4D-E). The relative expression of cleaved caspase-1, NLRP3, ASC, GSDMD-Nand IL-1β remained unchanged between the LPS (0.1 μg/mL)+pcDNA and LPS (0.1 μg/mL) groups ($P > 0.05$). However, the above indexes in the LPS (0.1 μg/mL)+NLRP3 group were memorably higher than those in LPS (0.1 μg/mL)+pcDNA group ($p < 0.001$), suggesting that overexpression of NLRP3 promoted the activation of this pathway. The relative expression of these proteins were markedly reduced following RE treatment ($p < 0.001$), which were partially reversed by over expression of NLRP3 ($p < 0.05$ or $p < 0.01$). In conclusion, RE inhibits pyroptosis by restraining NLRP3/Caspase-1/GSDMD pathway.

Over expression of NLRP3 reverses the inhibitory effect of RE on LX-2 cell activation

Finally, rescue experiments were performed to verify whether RE inhibited pyroptosis by restraining the NLRP3/Caspase-1/GSDMD pathway, thereby inhibiting LX-2 cell activation. The protein expression of fibronectin,

collagen Type Iand α-SMA in cells was detected by WB. The results suggested that the expression of above proteins in LPS (0.1 μg/mL)+NLRP3 group were dramatically greater than those in the LPS (0.1 μg/mL)+pcDNA group ($p < 0.001$) (fig. 5A-B), suggesting that NLRP3 over expression facilitated the activation of LX-2 cells. RE markedly reduced cell activation ($p < 0.001$), but this effect was counteracted by NLRP3 over expression ($p < 0.05$ or $p < 0.01$). These results demonstrate that RE inhibits pyroptosis by restraining the NLRP3/Caspase-1/GSDMD pathway, thereby hindering the activation of LX-2 cells.

DISCUSSION

Chronic liver disease affects 844 million people globally and causes approximately 2 million deaths each year, with cirrhosis responsible for half of these fatalities (Asrani *et al*., 2019; Marcellin and Kutala, 2018). LF represents a common pathological stage in numerous chronic liver conditions, including alcoholic liver disease. If the disease is not controlled, HSC activation can be continuously stimulated. The activated HSC have a strong protein synthesis capacity and can express a large amount of α-SMA, resulting in the formation of myofibroblasts, which can generate collagen fibers that are deposited in the extracellular interstitial tissue and form fiber scars and eventually grow into liver cancer and cirrhosis, which pose a major hazard to human health (Higashi *et al*., 2017; Kisseleva and Brenner, 2021; Lo and Kim, 2017). LF is also an inflammatory disease, which is accompanied by the secretion of a large number of inflammatory mediators during the occurrence of LF. Consequently, regulating the activation and proliferation of HSC or promoting their death and inhibiting inflammation are the main goals for reversing LF (Hammerich and Tacke, 2023). RE is an anesthetic that can be used in the anesthetic management of patients with cirrhosis. A recent study has revealed that RE reduces inflammation in bronchial pneumonia by inhibiting NLRP3 activity through PDPK1 ubiquitination (Yang and Li, 2024).

While RE has been shown to inhibit glioma cell growth and induce apoptosis by suppressing the NF-κB pathway (Xu *et al*., 2021), its role in LF remains unexplored. Therefore, this study aimed to establish an HSC activation model by employing varying concentrations of LPS, with the most effective concentration of LPS determined as 0.1 μg/mL. Following treatment of LX-2 cells with varying concentrations of RE, the viability of LX-2 cells was significantly inhibited by 20, 50and 100 μM RE and the protein expression of fibronectin, collagen Type I and α-SMA were decreased. These findings indicate that RE can suppress LX-2 cell activation and 100 μM RE has the strongest inhibitory effect.

Previous studies have demonstrated that the occurrence and development of LF are related to pyroptosis and inflammatory responses mediated by NLPR3 inflammatory mediators. On the one hand, the biological effects of IL-1β and IL-18 aggravate liver inflammation. On the other hand, the biological effects of GSDMD-N cause or aggravate liver pyroptosis, which together to aggravate liver injury and promote LF progression (de Carvalho Ribeiro and Szabo, 2022; Gao *et al*., 2021; Mridha *et al*., 2017). Consistent with these findings, we found that LPS-induced HSC exhibited swelling, irregular contraction patterns, irregular cell morphology, unclear nuclei and a large number of dead cells. Simultaneously, in contrast to the control group, the IL-1β and IL-18 levels in the model group were significantly elevated. Additionally, WB analysis was used to assess the expression of proteins in NLRP3/Caspase-1/GSDMD pathway to further confirm NLRP3's involvement in the activation of LX-2 cells.

Our findings demonstrate that LPS induces pyroptosis in LX-2 cells, as evidenced by significant activation of the NLRP3/Caspase-1/GSDMD pathway in model group compared to the control group. At the same time, LPS-stimulated LX-2 cells were treated with 100 μM RE and it was found that RE inhibited LDH release and NLRP3/Caspase-1/GSDMD pathway activation.

To further investigate whether RE can inhibit LX-2 cell activation by inhibiting NLRP3-mediated pyroptosis, we performed rescue experiments by over expressing the NLRP3 gene in cells. The results showed that NLRP3 over expression could promote LPS-induced cell activation and pyroptosis, which was completely opposite to RE and the inhibitory impact of RE on cell activation and pyroptosis was abolished by NLRP3 over expression.

CONCLUSION

Taken together, our results support our hypothesis that that RE prevents pyroptosis by blocking the NLRP3/Caspase-1/GSDMD pathway, thereby reducing LX-2 cell activation. These findings provide the first evidence that RE's anti-fibrotic activity involves modulation of the pyroptotic pathway in HSC, suggesting its potential as a therapeutic agent for LF.

Availability of data and materials

All data generated or analyzed during this study are included in this published article (and its supplementary information files).

Conflict of interest

The authors declare no competing interests.

REFERENCES

Asrani SK, Devarbhavi H, Eaton J and Kamath PS (2019). Burden of liver diseases in the world. *J. Hepatol.,* **70**: 151-171.

Babuta M, Morel C, de Carvalho Ribeiro M, Calenda C, Ortega-Ribera M, Thevkar Nagesh P, Copeland C, Zhuang Y, Wang Y, Cho Y, Joshi R, Brezani V, Hawryluk D, Datta AA, Mehta J, Nasser I and Szabo G (2024). Neutrophil extracellular traps activate hepatic stellate cells and monocytes via NLRP3 sensing in alcohol-induced acceleration of MASH fibrosis. *Gut.,* **73**: 1854-1869.

Buakaew W, Krobthong S, Yingchutrakul Y, Potup P, Thongsri Y, Daowtak K, Ferrante A and Usuwanthim K (2024). Investigating the antifibrotic effects of β-citronellol on a TGF-β1-stimulated LX-2 hepatic stellate cell model. *Biomolecules.,* **14**: 800.

Campana L, Esser H, Huch M and Forbes S (2021). Liver regeneration and inflammation: From fundamental science to clinical applications. *Nat. Rev. Mol. Cell. Biol.,* **22**: 608-624.

Ceccarelli S, Panera N, Mina M, Gnani D, De Stefanis C, Crudele A, Rychlicki C, Petrini S, Bruscalupi G, Agostinelli L, Stronati L, Cucchiara S, Musso G, Furlanello C, Svegliati-Baroni G, Nobili V and Alisi A (2015). LPS-induced TNF-α factor mediates pro-inflammatory and pro-fibrogenic pattern in non-alcoholic fatty liver disease. *Oncotarget.,* **6**: 41434-41452.

De Carvalho Ribeiro M and Szabo G (2022). Role of the inflammasome in liver disease. *Annu. Rev. Pathol.,* **17**: 345-365.

Fang H, Zhang Y, Wang J, Li L, An S, Huang Q, Chen Z, Yang H, Wu J and Zeng Z (2021). Remimazolam reduces sepsis-associated acute liver injury by activation of peripheral benzodiazepine receptors and p38 inhibition of macrophages. *Int. Immunopharmacol.,* **101**: 108331.

Fouts DE, Torralba M, Nelson KE, Brenner DA and Schnabl B (2012). Bacterial translocation and changes in the intestinal microbiome in mouse models of liver disease. *J. Hepatol.,* **56**: 1283-1292.

Gao X, Liu S, Tan L, Ding C, Fan W, Gao Z, Li M, Tang Z, Wu Y, Xu L, Yan L, Luo Y and Song S (2021). Estrogen receptor α regulates metabolic-associated fatty liver disease by targeting NLRP3-GSDMD axis-mediated hepatocyte pyroptosis. *J. Agric. Food. Chem.* **69**: 14544-14556.

Guo H, Xie M, Zhou C and Zheng M (2019). The relevance of pyroptosis in the pathogenesis of liver diseases. *Life. Sci.,* **223**: 69-73.

Hammerich L and Tacke F (2023). Hepatic inflammatory responses in liver fibrosis. *Nat. Rev. Gastroenterol. Hepatol.,* **20**: 633-646.

Hernaez R, Liu Y, Kramer JR, Rana A, El-Serag HB and Kanwal F (2020). Model for end-stage liver disease-sodium underestimates 90-day mortality risk in patients with acute-on-chronic liver failure. *J. Hepatol.,* **73**: 1425-1433.

Higashi T, Friedman SL and Hoshida Y (2017). Hepatic stellate cells as key target in liver fibrosis. *Adv. Drug. Deliv. Rev.,* **121**: 27-42.

Khanam A, Saleeb PG and Kottilil S (2021). Pathophysiology and treatment options for hepatic fibrosis: Can It be completely cured? *Cells.,* **10**: 1097.

Kisseleva T and Brenner D (2021). Molecular and cellular mechanisms of liver fibrosis and its regression. *Nat. Rev. Gastroenterol. Hepatol.,* **18**: 151-166.

Knorr J, Wree A and Feldstein AE (2022). Pyroptosis in steatohepatitis and liver diseases. *J. Mol. Biol.,* **434**: 167271.

Kui L, Kim AD, Onyuru J, Hoffman HM and Feldstein AE (2024). BRP39 regulates neutrophil recruitment in NLRP3 inflammasome-induced liver inflammation. *Cell. Mol. Gastroenterol. Hepatol.,* **17**: 481-497.

Lamkanfi M and Dixit VM (2014). Mechanisms and functions of inflammasomes. *Cell.,* **157**: 1013-1022.

Lee A and Shirley M (2021). Remimazolam: A review in procedural sedation. *Drugs.,* **81**: 1193-1201.

Liu X, Lin S, Zhong Y, Shen J, Zhang X, Luo S, Huang L, Zhang L, Zhou S and Tang J (2021). Remimazolam protects against LPS-induced endotoxicity improving survival of endotoxemia Mice. *Front. Pharmacol.,* **12**: 739603.

Liu Y, Kong X, You Y, Xiang L, Zhang Y, Wu R, Zhou L and Duan L (2022). S100A8-Mediated NLRP3 Inflammasome-dependent pyroptosis in macrophages facilitates liver fibrosis progression. Cells., **11**: 3579.

Lo RC and Kim H (2017). Histopathological evaluation of liver fibrosis and cirrhosis regression. *Clin. Mol. Hepatol.,* **23**: 302-307.

Marcellin P and Kutala BK (2018). Liver diseases: A major, neglected global public health problem requiring urgent actions and large-scale screening. *Liver. Int.,* **38** Suppl 1: 2-6.

Mridha AR, Wree A, Robertson AAB, Yeh MM, Johnson CD, Van Rooyen DM, Haczeyni F, Teoh NC, Savard C, Ioannou GN, Masters SL, Schroder K, Cooper MA, Feldstein AE and Farrell GC (2017). NLRP3 inflammasome blockade reduces liver inflammation and fibrosis in experimental NASH in mice. *J. Hepatol.,* **66**: 1037-1046.

Murao A, Aziz M, Wang H, Brenner M and Wang P (2021). Release mechanisms of major DAMPs. *Apoptosis.,* **26**: 152-162.

Onoda A and Suzuki Y (2022). A new anesthetic, remimazolam, is useful in the management of anesthesia in patients with liver cirrhosis. *Case. Rep. Anesthesiol.,* 9268454.

Ran Y, Su W, Gao F, Ding Z, Yang S, Ye L, Chen X, Tian G, Xi J and Liu Z (2021). Curcumin ameliorates white matter injury after ischemic stroke by inhibiting microglia/macrophage pyroptosis through nf-κb suppression and NLRP3 inflammasome inhibition. *Oxid. Med. Cell. Longev.,* 2021: 1552127.

Shi M, Chen J, Liu T, Dai W, Zhou Z, Chen L and Xie Y (2022). Protective effects of remimazolam on cerebral ischemia/reperfusion injury in rats by inhibiting of nlrp3

inflammasome-dependent pyroptosis. *Drug. Des. Devel. Ther.,* **16**: 413-423.

Shojaie L, Iorga A and Dara L (2020). Cell Death in Liver Diseases: A review. *Int. J. Mol. Sci.,* **21**: 9682.

Song J, Yu W, Chen S, Huang J, Zhou C and Liang H (2024). Remimazolam attenuates inflammation and kidney fibrosis following folic acid injury. *Eur. J. Pharmacol.,* **966**: 176342.

Wesolowski AM, Zaccagnino MP, Malapero RJ, Kaye AD and Urman RD (2016). Remimazolam: Pharmacologic considerations and clinical role in anesthesiology. *Pharmacotherapy.,* **36**: 1021-1027.

Xu W, Hu J, Liu W, Zhu Q, Gong X, Zhu P, Yang X, Xia R and Xue R (2021). Remimazolan inhibits glioma cell growth and induces apoptosis through down-regulation of NF-κB pathway. *IUBMB. Life.,* **73**: 341-348.

Yang M and Li L (2024). Remimazolam attenuates inflammation in bronchopneumonia through the inhibition of NLRP3 activity by PDPK1 ubiquitination. *Chem. Biol. Drug. Des.,* **103**: e14438.

Zhang Y, Zhang H, Li S, Huang K, Jiang L and Wang Y (2022). Metformin alleviates LPS-induced acute lung injury by regulating the SIRT1/NF-κB/NLRP3 pathway and inhibiting endothelial cell pyroptosis. *Front. Pharmacol.,* **13**: 801337.

Zhao J, Han M, Zhou L, Liang P, Wang Y, Feng S, Lu H, Yuan X, Han K, Chen X, Liu S and Cheng J (2020). TAF and TDF attenuate liver fibrosis through NS5ATP9, TGFβ1/Smad3and NF-κB/NLRP3 inflammasome signaling pathways. *Hepatol. Int.,* **14**: 145-160.

Zhao YQ, Deng XW, Xu GQ, Lin J, Lu HZ and Chen J (2023). Mechanical homeostasis imbalance in hepatic stellate cells activation and hepatic fibrosis. *Front. Mol. Biosci.,* **10**: 1183808.